Phase Transitions with Semi-Diffuse Interfaces

James M. Greenberg[1]
Department of Mathematical Sciences
Carnegie Mellon University
Pittsburgh, PA 15213
greenber@andrew.cmu.edu

Abstract

In this paper we examine new "phase-field" models with semi-diffuse interfaces. These models have the property that the $-1/+1$ planar phase transitions take place over a finite interval. The models also support multiple interface solutions with interfaces centered at arbitrary points $L_1 < L_2 < \ldots < L_N$. These solutions correspond to local minima of an entropy functional (see (3.3) and (3.7)) rather than saddle points and are dynamically stable. The classical models have no such exact solutions but they do support solutions with N equally spaced transition points where the order parameter transitions between valves $p_{\min}(N)$ and $p_{\max}(N)$ satisfying $-1 < p_{\min}(N) < 0 < p_{\max}(N) < 1$. These solutions of the classical model are saddle points of the entropy functional associated with those models and are not dynamically stable.

1 Introduction

In classical "phase-field" models used to describe melting and solidification planar phase transitions where the order parameter p goes from -1 to $+1$ are typically of the form

$$p = \tanh\left(\frac{x-L}{\delta}\right).$$

These transitions are diffuse and require the whole interval $-\infty < x < \infty$ to complete. The parameter L where $p = 0$ is identified as the position of the interface.

In this paper we examine a new class of "phase-field" models with semi-diffuse interfaces. These models have the property that the $-1/+1$ planar transitions take place over a finite interval; i.e. the order parameter p satisfies

[1]This research was partially supported by the Applied Mathematical Sciences Program, U.S. Department of Energy and by the U.S. National Science Foundation.

$$p = \begin{cases} -1, & x \leq L - \delta\Omega \\ 0, & x = L \\ 1, & L + \delta\Omega \leq x, \end{cases}$$

$p(-x) = -p(x)$, and $0 < p'(x),\ L - \delta\Omega < x < L + \delta\Omega$. Ω is independent of the length scale δ and is determined by other system parameters. These models also support multiple interface solutions with interfaces centered at $L_1 < L_2 < \ldots L_N$. These solutions are valid so long as $L_{i+1} - L_i > 2\delta\Omega$, $1 \leq i \leq N-1$. The classical models have no such exact solutions. We note these solutions are local minima of the entropy functional which characterizes the system and are dynamically stable.

In section 2 we present the new model in the context of melting and solidification problems and establish a decay estimate for the system which allows us to replace the detailed energy balance with an averaged energy balance. This replacement yields a non-local equation for the order parameter p rather than a coupled system linking the temperature and order parameter. In section 3 we establish the existence of multiple moving front solutions to this non-local equation and the convergence of these solutions to equilibria exhibiting microstructure. In section 3 we also show that if certain parameter constraints hold, then the system supports a Gibbs-Thomson relation similar to the classical "phase-field" model. Section 4 is devoted to numerical simulations.

2 The Model and Basic Estimates

In this section we focus on a new phase-field model with semi-diffuse interfaces which we use to describe melting and solidification processes. Our notation is as follows:

θ ... denotes the absolute temperature,

θ_m ... denotes the nominal melt temperature of the material,

$T = \dfrac{\theta - \theta_m}{\theta_m}$ ... is the dimensionless temperature field,

p ... is the dimensionless order parameter which characterizes whether the material is in the solid or liquid state (when $p = -1$ we have a pure solid and when $p = +1$ a pure liquid), and

e ... is the dimensionless internal energy density.

We assume that

$$e = T + e_\mu(p) \tag{2.1}$$

where

$$e_\mu(p) = \int_0^p |1 - s^2|^\mu ds \tag{2.2}$$

and $0 < \mu < 1$. Conservation of energy takes the form

$$\tau_1 e_t + l_1 \text{ div } \boldsymbol{q} = 0 \Leftrightarrow \tau_1(T_t + |1-p^2|^\mu p_t) + l_1 \text{ div } \boldsymbol{q} = 0 \tag{2.3}$$

where $\tau_1 > 0$ is interpreted as a relaxation time, $l_1 > 0$ a diffusive length scale, and $\boldsymbol{q}$ is the dimensionless heat flux vector. The heat flux $\boldsymbol{q}$ is related to T via either the Fourier Law

$$\boldsymbol{q} = -\alpha^2 l_1 \nabla T \tag{2.4.a}$$

or the relaxation equation

$$\tau_1 \boldsymbol{q}_t + \boldsymbol{q} + \alpha^2 l_1 \nabla T = 0. \tag{2.4.b}$$

In either case $\alpha^2 > 0$ is a dimensionless parameter.

We assume the order parameter p is linked to T via

$$\frac{\delta}{c} p_t = \delta^{\gamma+1} \text{ div } \left(|\nabla p|^{\gamma-1} \nabla p \right) + T|1-p^2|^\mu + p|1-p^2|^\lambda \text{ sign } (1-p^2). \tag{2.5}$$

Here $\delta > 0$ has the interpretation of the diffusive length scale for the p process, c has the dimensions of length/time, and we assume that

$$1 \leq \gamma \quad , \quad 0 < \mu < 1 \quad , \quad \text{and } 0 \leq \lambda < 1. \tag{2.6}$$

It is hard to argue on fundamental grounds for the value of the models put forth here over those popularized by others. All such models are phenomenological, consistent with continuum thermodynamics, and represent an attempt to avoid the difficulties of dealing with discontinuities in the internal energy present in the sharp interface theories of melting and solidification. The strength of any such model lies in its predictions and whether these conform with what is observed. The models developed here seem to meet that test and, as the reader shall see, they are fairly easy to deal with analytically.

To obtain the multiple moving front solutions described in the introduction not all parameter choices satisfying (2.6) are permissible, the parameters must satisfy the additional constraint that

$$(\gamma + 1)\mu = \lambda + 1. \tag{2.7}$$

If one also desires a Gibbs-Thomson relation to hold in the $\delta = 0^+$ sharp interface limit, one is further required to choose $\gamma = 1$. This choice and (2.7) then constrains μ to satisfy

$$\mu = \frac{\lambda + 1}{2}. \tag{2.8}$$

None of the constraints (2.7) or (2.8) are necessary for the basic decay estimates which we shall develop presently. We note that the classical phase-field models all deal with the situation where $\gamma = 1$ and μ and λ are both positive integers; for details see [1-10].

Throughout the remainder of this section we assume that (2.3), (2.4.a) or (2.4.b), and (2.5) hold in a bounded, simply connected domain Ω in R^2 with smooth boundary $\partial\Omega$. On $\partial\Omega$ we assume that

$$\boldsymbol{q} \cdot \boldsymbol{n} = \nabla p \cdot \boldsymbol{n} = 0 \quad , \quad (x, y) \in \partial\Omega \; \& \; t > 0. \tag{2.9}$$

Here, $\boldsymbol{n}(x, y)$ is the exterior unit normal to $\partial\Omega$ at (x, y).

If $\boldsymbol{q}$ is given by (2.4.b) in $\Omega \times (0,\infty)$, we assume that the initial data for $\boldsymbol{q}$ satisfies curl $\boldsymbol{q}(x,y,0^+) = \boldsymbol{e}_3(q_{2x} - q_{1y})(x,y,0^+) \equiv 0$. This hypothesis guarantees the existence of a potential ϕ so that

$$\boldsymbol{q} = -\alpha^2 l_1 \nabla\phi \quad , \quad (x,y) \in \Omega \ \& \ t \geq 0 \tag{2.10}$$

and

$$T = \tau_1 \phi_t + \phi \qquad (x,y) \in \Omega \ \& \ t \geq 0. \tag{2.11}$$

In this situation, (2.3) reduces to

$$\tau_1(\tau_1\phi_t + \phi)_t + \tau_1|1-p^2|^\mu p_t - \alpha^2 l_1^2 \Delta\phi = 0 \quad , \quad (x,y) \in \Omega \ \& \ t > 0 \tag{2.12}$$

and (2.9) and (2.10) imply that

$$\nabla\phi \cdot \boldsymbol{n} = 0 \quad , \quad (x,y) \in \partial\Omega \ \& \ t > 0. \tag{2.13}$$

On the other hand if $\boldsymbol{q}$ is given by (2.4.a), then (2.3) reduces to

$$\tau_1(T_t + |1-p^2|^\mu p_t) - \alpha^2 l_1^2 \Delta T = 0 \quad , \quad (x,y) \in \Omega \ \& \ t \geq 0 \tag{2.14}$$

and (2.9) implies that

$$\nabla T \cdot \boldsymbol{n} = 0 \quad , \quad (x,y) \in \partial\Omega \ \& \ t > 0. \tag{2.15}$$

Basic Estimates

We first observe that if $-1 \leq p(x,y,0^+) \leq 1$, then the same inequality is valid for all $t \geq 0$. We next observe that if we multiply (2.5) by $-p_t/\delta$ we obtain

$$\frac{\partial}{\partial t}\left(\frac{|1-p^2|^{\lambda+1}}{2\delta(\lambda+1)} + \frac{\delta^\gamma |\nabla p|^{\gamma+1}}{(\gamma+1)}\right) - \delta^\gamma \text{ div } \left(p_t |\nabla p|^{\gamma-1}\nabla p\right) = -\frac{p_t^2}{c} + \frac{T|1-p^2|^\mu p_t}{\delta}. \tag{2.16}$$

If $\boldsymbol{q}$ is given by the Fourier Law (2.4.a), then multiplication of (2.14) by $\dfrac{T}{\tau_1\delta}$ yields

$$\frac{\partial}{\partial t}\left(\frac{T^2}{2\delta}\right) - \frac{\alpha^2 l_1^2}{\tau_1\delta} \text{ div } (T\nabla T) = -\frac{\alpha^2 l_1^2}{\tau_1\delta}|\nabla T|^2 - \frac{T|1-p^2|^\mu p_t}{\delta}, \tag{2.17}$$

while multiplication of (2.14) by $\dfrac{T_t}{\tau_1 c}$ yields

$$\frac{\alpha^2 l_1^2}{2\tau_1 c}\frac{\partial}{\partial t}(|\nabla T|^2) - \frac{\alpha^2 l_1^2}{\tau_1 c} \text{ div } (T_t \nabla T) = -\frac{T_t^2}{c} - \frac{|1-p^2|^\mu T_t p_t}{c}. \tag{2.18}$$

On the other hand, if $\boldsymbol{q}$ obeys the relaxation law (2.4.b), then multiplication of (2.12) by $\dfrac{T}{\tau_1\delta} = \dfrac{(\tau_1\phi_t + \phi)}{\tau_1\delta}$ yields

$$\frac{1}{2\delta}\frac{\partial}{\partial t}((\tau_1\phi_t+\phi)^2+\alpha^2 l_1^2|\nabla\phi|^2)-\frac{\alpha^2 l_1^2}{\tau_1\delta}\,\mathrm{div}\,((\tau_1\phi_t+\phi)\nabla\phi)=-\frac{\alpha^2 l_1^2}{\tau_1\delta}|\nabla\phi|^2-\frac{T|1-p^2|^\mu p_t}{\delta} \tag{2.19}$$

while multiplication of (2.12) by $\dfrac{\phi_t}{\tau_1 c}$ yields

$$\frac{1}{2}\frac{\partial}{\partial t}\left(\frac{\tau_1}{c}\phi_t^2+\frac{\alpha^2 l_1^2}{\tau_1 c}|\nabla\phi|^2\right)-\frac{\alpha^2 l_1^2}{\tau_1 c}\,\mathrm{div}\,(\phi_t\nabla\phi)=-\frac{\phi_t^2}{c}-\frac{|1-p^2|^\mu\phi_t p_t}{c}. \tag{2.20}$$

When the Fourier Law holds we add (2.16) - (2.18), integrate the resulting expression over $\Omega\times(0,t)$, and exploit the boundary conditions $(2.9)_2$ and (2.15) and the estimate $-1\le p\le 1$ to obtain

$$\begin{aligned}
&\iint\limits_\Omega\left(\frac{|1-p^2|^{\lambda+1}}{2\delta(\lambda+1)}+\frac{\delta^\gamma|\nabla p|^{\gamma+1}}{(\gamma+1)}+\frac{T^2}{2\delta}+\frac{\alpha^2 l_1^2}{2\tau_1 c}|\nabla T|^2\right)(x,y,t)dxdy\le\\
&\iint\limits_\Omega\left(\frac{|1-p^2|^{\lambda+1}}{2\delta(\lambda+1)}+\frac{\delta^\gamma|\nabla p|^{\gamma+1}}{(\gamma+1)}+\frac{T^2}{2\delta}+\frac{\alpha^2 l_1^2}{2\tau_1 c}|\nabla T|^2\right)(x,y,0^+)dxdy\\
&-\int_0^t\left(\iint\limits_\Omega\left(\frac{p_s^2+T_s^2}{2c}+\frac{\alpha^2 l_1^2}{\tau_1\delta}|\nabla T|^2\right)(x,y,s)dxdy\right)ds.
\end{aligned} \tag{2.21}$$

The latter inequality implies, in particular, that ∇T is bounded in $L_2(\Omega)\cap L_2(\Omega\times(0,t))$ independently of t. We also have p_s and T_s bounded in $L_2(\Omega\times(0,t))$ independently of t.

Lemma 1. ∇T tends to zero strongly in $L_2(\Omega)$ as $t\to\infty$.

Proof. The preceding bounds imply that we can find an increasing sequence of times, $\{t_n\}_{n=1}^\infty$, so that $\lim\limits_{n\to\infty}t_n=\infty$ and $\lim\limits_{n\to\infty}\iint\limits_\Omega|\nabla T|^2(x,y,t_n)dxdy=0$. Moreover, (2.18) implies that for any $t<t_n$

$$\begin{aligned}
&\iint\limits_\Omega|\nabla T|^2(x,y,t)dxdy\le\iint\limits_\Omega|\nabla T|^2(x,y,t_n)dxdy\\
&+\frac{\tau_1}{\alpha^2 l_1^2}\int_t^{t_n}\left(\iint\limits_\Omega(3T_s^2+p_s^2)(x,y,s)dxdy\right)ds.
\end{aligned} \tag{2.22}$$

If we now let $n\to\infty$ and exploit the fact that T_t and p_t are $L_2(\Omega\times(0,\infty))$ we obtain

$$\iint\limits_\Omega|\nabla T|^2(x,y,t)dxdy\le\frac{\tau_1}{\alpha^2 l_1^2}\int_t^\infty\left(\iint\limits_\Omega(3T_s^2+p_s^2)(x,y,s)dxdy\right)ds. \tag{2.23}$$

(2.23) then yields the desired result. ■

When $\boldsymbol{q}$ obeys the relaxation law (2.4.b) we add (2.16), (2.19), and (2.20), integrate the resulting expression over $\Omega \times (0,t)$, and exploit the boundary conditions $(2.9)_2$ and (2.13) and the estimate $-1 \leq p \leq 1$ to obtain

$$\iint\limits_{\Omega} \left(\frac{|1-p^2|^{\lambda+1}}{2\delta(\lambda+1)} + \frac{\delta^{\gamma}|\nabla p|^{\gamma+1}}{(\gamma+1)} + \frac{(\tau_1\phi_t+\phi)^2}{2\delta} + \frac{\tau_1}{2c}\phi_t^2 + \frac{\alpha^2 l_1^2}{2}\left(\frac{1}{\delta}+\frac{1}{\tau_1 c}\right)|\nabla\phi|^2 \right)(x,y,t)dxdy$$

$$\leq \iint\limits_{\Omega} \left(\frac{|1-p^2|^{\lambda+1}}{2\delta(\lambda+1)} + \frac{\delta^{2}|\nabla p|^{\gamma+1}}{(\gamma+1)} + \frac{(\tau_1\phi_t+\phi)^2}{2\delta} + \frac{\tau_1\phi_t^2}{2c} + \frac{\alpha^2 l_1^2}{2}\left(\frac{1}{\delta}+\frac{1}{\tau_1 c}\right)|\nabla\phi|^2 \right)(x,y,0^+)dxdy$$

$$-\int_0^t \left(\iint\limits_{\Omega} \left(\frac{p_s^2+\phi_s^2)}{2c} + \frac{\alpha^2 l_1^2}{\tau_1\delta}|\nabla\phi|^2 \right)(x,y,s)dxdy \right) ds. \tag{2.24}$$

The latter inequality implies that $\nabla\phi$ and ϕ_t are bounded in $L_2(\Omega) \cap L_2(\Omega \times (0,t))$ independently of t. We also have p_s bounded in $L_2(\Omega \times (0,t))$ independently of t.

Lemma 2. The potential ϕ satisfies

$$\lim_{t\to\infty} \iint\limits_{\Omega} \left(\tau_1\phi_t^2 + \frac{\alpha^2 l_1^2}{\tau_1}|\nabla\phi|^2 \right)(x,y,t)dxdy = 0. \tag{2.25}$$

Proof. The inequality (2.24) implies we can find a sequence $t_n < t_{n+1}$, $n = 1, 2, \ldots$, with $\lim\limits_{n\to\infty} t_n = \infty$ so that

$$\lim_{n\to\infty} \iint\limits_{\Omega} \left(\tau_1\phi_t^2 + \frac{\alpha^2 l_1^2}{\tau_1}|\nabla\phi|^2 \right)(x,y,t_n)dxdy = 0. \tag{2.26}$$

(2.20) and the inequalities $-1 \leq p \leq 1$ imply that for any $t < t_n$

$$\iint\limits_{\Omega} \left(\tau_1\phi_t^2 + \frac{\alpha^2 l_1^2}{\tau_1}|\nabla\phi|^2 \right)(x,y,t)dxdy \leq \iint\limits_{\Omega} \left(\tau_1\phi_t^2 + \frac{\alpha^2 l_1^2}{\tau_1}|\nabla\phi|^2 \right)(x,y,t_n)dxdy$$

$$+\int_t^{t_n} \left(\iint\limits_{\Omega} \left(3\phi_s^2 + p_s^2\right)(x,y,s)dxdy \right) ds. \tag{2.27}$$

If we now let $n \to \infty$ and exploit the fact that (2.24) implies that p_s and ϕ_s are in $L_2(\Omega \times (0,\infty))$ we obtain

$$\iint\limits_{\Omega} \left(\tau_1\phi_t^2 + \frac{\alpha^2 l_1^2}{\tau_1}|\nabla\phi|^2 \right)(x,y,t)dxdy \leq \int_t^{\infty} \left(\iint\limits_{\Omega} \left(3\phi_s^2 + p_s^2\right)(x,y,s)dxdy \right) ds \tag{2.28}$$

and (2.28) implies (2.25) ■

No matter whether the heat flux $\boldsymbol{q}$ is given by (2.4.a) or (2.4.b), the results of Lemmas 1 and 2 guarantee that if we make the following decomposition of the temperature field

$$T(x,y,t) = T_0(t) + T_1(x,y,t) \tag{2.29}$$

where

$$\iint\limits_{\Omega} T_1(x,y,t)dxdy = 0 \quad , \quad t \geq 0, \tag{2.30}$$

then the spatially varying temperature field T_1, converges to zero strongly in $L_2(\Omega)$ as $t \to \infty$. When $\boldsymbol{q}$ is given by (2.4.a) we obtain the stronger result that T_1 converges to zero strongly in $H_1(\Omega)$ as $t \to \infty$.

These observations imply that if our interest is in the long term dynamics of the system we may neglect the detailed energy balance (2.3) and (2.4.a) or (2.4.b) and replace the term $T|1-p^2|^\mu$ in (2.5) by $T_0|1-p^2|^\mu$ where

$$T_0(t) = \left(e_\mu(1)H_0 - \iint\limits_{\Omega} e_\mu(p(x,y,t))dxdy \right) / \iint\limits_{\Omega} 1dxdy \tag{2.31}$$

and the constant H_0 is given by

$$H_0 = \left(\iint\limits_{\Omega} (T(x,y,0^+) + e_\mu(p(x,y,0^+)))dxdy \right) /e_\mu(1). \tag{2.32}$$

3 Moving Front Solutions

In this section we produce the moving front solutions discussed in the introduction. These satisfy the reduced one-dimensional equation

$$\frac{\delta}{c}p_t = \delta^{\gamma+1}\frac{\partial}{\partial x}\left(|p_x|^{\gamma-1}p_x\right) + T_0(t)\left|1-p^2\right|^\mu + p\left|1-p^2\right|^\lambda \text{ sign } (1-p^2), \; 0<x<1 \tag{3.1}$$

and boundary conditions

$$\frac{\partial p}{\partial x}(0,t) = \frac{\partial p}{\partial x}(1,t) = 0. \tag{3.2}$$

Here,

$$T_0(t) = e_\mu(1)H_0 - \int_0^1 e_\mu(p(x,t))dx, \tag{3.3}$$

$$H_0 = \left(\int_0^1 (T(x, 0^+) + e_\mu(p(x, 0^+)))dx \right) / e_\mu(1) \tag{3.4}$$

and

$$e_\mu(p) = \int_0^p |1 - s^2|^\mu ds. \tag{3.5}$$

Our justification for replacing the detailed energy balance (2.3) and either (2.4.a) or (2.4.b) with (3.3) is the decay estimate of the last section which guarantees that the spatially varying component of the temperature decays to zero.

We note that solutions of (3.1) - (3.5) are gradient flows; i.e. for every $\phi \in C^1[0, 1]$

$$\int_0^1 \phi(x) p_t(x, t) dx = -cD\mathcal{J}(p|\phi) \tag{3.6}$$

where

$$\mathcal{J}(p) = \int_0^1 \left(\frac{\delta^\gamma |p_x|^{\gamma+1}}{(\gamma + 1)} + \frac{|1 - p^2|^{\lambda+1}}{2\delta(\lambda + 1)} \right) (x, t) dx + \frac{T_0^2(t)}{2\delta}, \tag{3.7}$$

$T_0(t) = T_0(p)(t)$ is given by (3.3), and finally

$$D\mathcal{J}(p|\phi) = \int_0^1 \left(\delta^\gamma |p_x|^{\gamma-1} p_x \phi_x - \frac{p|1 - p^2|^\lambda}{\delta} \text{ sign } (1 - p^2)\phi \right) (x, t) dx - \frac{T_0(t)}{\delta} \int_0^1 \left(|1 - p^2|^\mu \phi \right) (x, t) dx, \tag{3.8}$$

or

$$D\mathcal{J}(p|\phi) = -\int_0^1 \left(\phi \left(\frac{\partial}{\partial x} \left(\delta^\gamma |p_x|^{\gamma-1} p_x \right) + \frac{p|1 - p^2|^\lambda |\text{sign } (1 - p^2) + T_0|1 - p^2|^\mu}{\delta} \right) \right) (x, t) dx. \tag{3.9}$$

We'll return to these identities at the end of this section.

We also require that the parameters $\gamma \geq 1$, $0 < \mu < 1$, and $0 \leq \lambda < 1$ satisfy (2.7).

The moving front solutions will be a concatintion of a basic profile, $\tilde{p}$, of the form:

$$p_N(x,t) = \pm \begin{cases} -1,\ 0 \le x \le L_1(t) - \Omega\delta \\ \tilde{p}\left(\dfrac{x - L_1(t)}{\delta}\right),\ L_1(t) - \Omega\delta < x < L_1(t) + \Omega\delta \\ 1,\ L_1(t) + \Omega\delta \le x \le L_2(t) - \Omega\delta \\ \vdots \\ (-1)^k,\ L_{k-1}(t) + \Omega\delta \le x \le L_k(t) - \Omega\delta \\ (-1)^{k-1}\tilde{p}\left(\dfrac{x - L_k(t)}{\delta}\right),\ L_k(t) - \Omega\delta < x < L_k(t) + \Omega\delta, 2 \le k \le N-1 \\ \vdots \\ (-1)^N,\ L_{N-1}(t) + \Omega\delta \le x \le L_N(t) - \Omega\delta \\ (-1)^{N-1}\tilde{p}\left(\dfrac{x - L_N(t)}{\delta}\right),\ L_N(t) - \Omega\delta < x < L_N(t) + \Omega\delta, \\ (-1)^{N+1},\ L_N(t) + \Omega\delta \le x \le 1. \end{cases} \tag{3.10}$$

Each of the odd indexed interfaces move at a common speed $\dfrac{dL}{dt}$; i.e.

$$\frac{dL_{2i-1}}{dt}(t) = \frac{dL}{dt}(t), \tag{3.11}$$

the even indexed interfaces satisfy

$$\frac{dL_{2i}}{dt}(t) = -\frac{dL}{dt}(t), \tag{3.12}$$

and finally the basic profile satisfies

$$\frac{d}{d\xi}\left(|\tilde{p}_\xi|^{\gamma-1}\tilde{p}_\xi\right) + \frac{\dot{L}}{c}(t)\tilde{p}_\xi + T_0(t)\left|1 - \tilde{p}^2\right|^\mu + \tilde{p}\left|1 - \tilde{p}^2\right|^\lambda \text{ sign } \left(1 - \tilde{p}^2\right) = 0. \tag{3.13}$$

That this equation must hold comes from insertion of (3.10) into (3.1). We seek a solution to (3.13) satisfying the reduced ansatz

$$\frac{d\tilde{p}}{d\xi} = A\left|1 - \tilde{p}^2\right|^\mu \tag{3.14}$$

where $0 < \mu < 1$, $A > 0$ and $\tilde{p}(0) = 0$. The reduced ansatz implies that

$$|\tilde{p}_\xi|^{\gamma-1}\tilde{p}_\xi = A^\gamma\left|1 - \tilde{p}^2\right|^{\gamma\mu} \tag{3.15}$$

and

$$\frac{d}{d\xi}\left(|\tilde{p}_\xi|^{\gamma-1}\tilde{p}_\xi\right) = -2\gamma\mu A^{\gamma+1}\tilde{p}\left|1-\tilde{p}^2\right|^{(\gamma+1)\mu-1} \text{ sign } (1-\tilde{p}^2) \tag{3.16}$$

and therefore (3.13) reduces to

$$\left(-2\gamma\mu A^{\gamma+1}\tilde{p}|1-\tilde{p}^2|^{(\gamma+1)\mu-1} + \tilde{p}|1-\tilde{p}^2|^{\lambda}\right) \text{ sign } \left(1-\tilde{p}^2\right) + \left(\frac{\dot{L}A}{c} + T_0\right)|1-\tilde{p}^2|^{\mu} = 0 \tag{3.17}$$

The last equation implies that L must satisfy the kinetic relation

$$\frac{dL}{dt} = -\frac{-cT_0(t)}{A} \tag{3.18}$$

while (2.7) implies that

$$(\gamma+1)\mu - 1 = \lambda \tag{3.19}$$

and thus (3.17) holds provided

$$A = \left(\frac{1}{2(\lambda+1-\mu)}\right)^{\frac{\mu}{\lambda+1}}. \tag{3.20}$$

Finally, the basic profile is given by the quadrature formula

$$(2(\lambda+1-\mu))^{\frac{\mu}{\lambda+1}} \int_0^{\tilde{p}(\xi)} \frac{d\eta}{(1-\eta^2)^{\mu}} = \xi \tag{3.21}$$

for $-\Omega < \xi < \Omega$ where Ω is defined by

$$(2(\lambda+1-\mu))^{\frac{\mu}{\lambda+1}} \int_0^{1} \frac{d\eta}{(1-\eta^2)^{\mu}} = \Omega. \tag{3.22}$$

For $\xi \le -\Omega$, $\tilde{p}(\xi) \equiv -1$ and for $\Omega \le \xi$, $\tilde{p}(\xi) = 1$. The fact that the basic profile is odd in ξ guarantees that the moving front solution defined in (3.10) satisfies

$$\int_0^1 e_\mu(p_N(x,t))dx = e_\mu(1)\left(\sum_{i=1}^{N/2+1}(L_{2i}-L_{2i-1}) - \sum_{i=1}^{[N/2]+1}(L_{2i-1}-L_{2(i-1)})\right). \tag{3.23}$$

In the above formula $[N/2]$ is the greatest integer which is less than or equal to $N/2$ and we have adopted the convention that $L_0(t) \equiv 0$ and that $L_{N+1}(t) \equiv 1$. An equivalent formula to (3.23) is

$$\int_0^1 e_\mu(p_N(x,t))dx = e_\mu(1)\left(1 - 2\sum_{i=1}^{[N/2]+1}\left(L_{2i-1}-L_{2(i-1)}\right)\right) \tag{3.24}$$

and the latter identity implies that so long as $\Omega\delta < L_1(t)$, $2\Omega\delta < L_{i+1}(t) - L_i(t)$, and $L_N(t) < 1 - \Omega\delta$, the temperature T_0 is given by

$$T_0(t) = e_\mu(1)\left(H_0 - 1 + 2\sum_{i=1}^{[N/2]+1}\big(L_{2i-1} - L_{2(i-1)}\big)\right). \tag{3.25}$$

Finally, the individual interfaces satisfy

$$\frac{dL_i}{dt} = (-1)^i c T_0(t)(2(\lambda+1-\mu))^{\frac{\mu}{\lambda+1}}. \tag{3.26}$$

The last identity implies that

$$\begin{aligned}\frac{d}{dt}\big(L_{2i-1} - L_{2(i-1)}\big) &= -2cT_0(2(\lambda+1-\mu))^{\frac{\mu}{\lambda+1}} = \\ 2ce_\mu(1)\,(2(\lambda+1-\mu))^{\frac{\mu}{\lambda+1}} &\left(1 - H_0 - 2\sum_{i=1}^{[N/2]+1}\big(L_{2i-1} - L_{2(i-1)}\big)\right)\end{aligned} \tag{3.27}$$

and thus that $\eta \stackrel{def}{=} \sum_{i=1}^{[N/2]+1}\big(L_{2i-1} - L_{2(i-1)}\big)$ obeys

$$\frac{d\eta}{dt} = ce_\mu(1)N(2(\lambda+1-\mu))^{\frac{\mu}{\lambda+1}}(1 - H_0 - 2\eta). \tag{3.28}$$

Given an initial distribution of internal interfaces $\{L_i^0\}_{i=1}^N$ satisfying

$$\Omega\delta < L_1^0,\ 2\Omega\delta < L_{i+1}^0 - L_i^0,\ 1 \le i \le N-1,\ \text{and}\ L_N^0 < 1 - \Omega\delta \tag{3.29}$$

we let

$$\eta^0 = \sum_{i=1}^{[N/2]+1}\big(L_{2i-1}^0 - L_{2(i-1)}^0\big) \tag{3.30}$$

and solve (3.28) to obtain

$$\eta(t) = \eta^0 e^{-2KNt} + (1 - H_0)(1 - e^{-2KNt})/2 \tag{3.31}$$

where

$$K = ce_\mu(1)(2(\lambda+1-\mu))^{\frac{\mu}{\lambda+1}}. \tag{3.32}$$

This latter formula implies that a **necessary condition** for (3.31) to be valid for all $t \ge 0$ is that the constant H_0 satisfies

$$-1 + 2N\Omega\delta < H_0 < 1 - 2N\Omega\delta. \tag{3.33}$$

If we assume that (3.33) holds, then the individual interfaces are given by

$$L_i(t) = L_i^0 + (-1)^{i-1}(1 - H_0 - 2\eta^0)(1 - e^{-2KNt})/2N \tag{3.34}$$

and, once again, a necessary condition for (3.34) to be valid for all $t \geq 0$ is that

$$\Omega\delta < L_1(t), 2\Omega\delta < L_{i+1}(t) - L_i(t),\ 1 \leq i \leq N-1,\ \text{and}\ L_N(t) < 1 - \Omega\delta. \tag{3.35}$$

We note that if we evaluate the functional $\mathcal{J}(\cdot)$ defined in (3.7) on the profile p_N defined in (3.10) we obtain

$$\mathcal{J}(p_N) = \frac{N 2^{\frac{\mu}{\lambda+1}}}{(\lambda+1-\mu)^{\frac{\lambda+1-\mu}{\lambda+1}}} \int_0^1 |1-p^2|^{\lambda+1-\mu} dp + \left(1 - H_0 - 2\sum_{i=1}^{[N/2]+1} \left(L_{2i-1} - L_{2(i-1)}\right)\right)^2 /2\delta. \tag{3.36}$$

The first term on the right hand side of (3.36) represents the integral

$$I \overset{def}{=} \int_0^1 \left(\frac{\delta^\gamma |\tilde{p}_{Nx}|^{\gamma+1}}{(\gamma+1)} + \frac{|1-\tilde{p}_N^2|^{\lambda+1}}{2\delta(\lambda+1)} \right)(x,t)dx$$

and is independent of the position of the particular interfaces $L_i, 1 \leq i \leq N$, so long as the constraints (3.35) hold. This observation implies that the equilibrium interfaces

$$L_i^\infty = L_i^0 + (-1)^{i-1}(1 - H_0 - 2\eta^0)/2N \tag{3.37}$$

and associated equilibrium profiles $p_N(\cdot,\infty)$ are local minima of $\mathcal{J}(\cdot)$ rather than saddle points.

Gibbs-Thomson Relation

We conclude this section with some remarks about the Gibbs-Thomson relation for the reduced 2-dimensional equation

$$\frac{\delta}{c} p_t = \delta^2 \Delta p + T_0(t)|1-p^2|^{\frac{1+\lambda}{2}} + p|1-p^2|^\lambda \text{ sign } (1-p^2). \tag{3.38}$$

Again, we assume this equation holds in a bounded, simply connected domain Ω in R^2 and on $\partial\Omega$ we require that

$$\frac{\partial p}{\partial n} = 0 \quad , \quad (x,y) \in \partial\Omega. \tag{3.39}$$

Here we have exploited the results of section 2 and replaced the balance of energy with the mean temperature model

$$T_0(t) = \left(e_{\frac{1+\lambda}{2}}(1)H_0 - \iint\limits_0 e_{\frac{1+\lambda}{2}}(p(x,y,t))dxdy \right) / \iint\limits_\Omega 1 dxdy \tag{3.40}$$

where

$$H_0 = \iint\limits_{\Omega} \Big(T(x,y,0^+) + e_{\frac{1+\lambda}{2}}(p(x,y,0^+)) \Big)\, dxdy / e_{\frac{1+\lambda}{2}}(1) \tag{3.41}$$

and

$$e_{\frac{1+\lambda}{2}}(p) = \int_0^p |1-s^2|^{\frac{1+\lambda}{2}} ds. \tag{3.42}$$

Our task is to find the analogue of the moving front solutions for (3.38) - (3.42). For simplicity we confine our attention to solutions with a single moving interface.

We assume that at some instant, t_0, the solution to (3.38) - (3.42) has the following structure: there exists a simple closed curve

$$\Gamma(t_0) = \{x = \hat{x}(s,t_0) \text{ and } y = \hat{y}(s,t_0),\ 0 \le s \le L(t_0)\} \tag{3.43}$$

in Ω with the property that $p < 0$ in the region surrounded by $\Gamma(t_0)$, $p(\hat{x}(s,t_0),\ \hat{y}(s,t_0),t_0) = 0$, and $p > 0$ in the portion of Ω exterior to $\Gamma(t_0)$. We further assume the curve $\Gamma(t_0)$ is parameterized by arc length; i.e. that $\hat{x}_s^2(s,t_0) + \hat{y}_s^2(s,t_0) = 1$. We let

$$\boldsymbol{t}(s,t_0) = (\hat{x}_s, \hat{y}_s)(s,t_0) \text{ and } \boldsymbol{n}(s,t_0) = (\hat{y}_s, -\hat{x}_s)(s,t_0) \tag{3.44}$$

be the unit tangent and normal to $\Gamma(t_0)$ at $(\hat{x},\hat{y})(s,t_0)$ and note that

$$\boldsymbol{n}_s(s,t_0) = K(s,t_0)\boldsymbol{t}(s,t_0) \tag{3.45}$$

and

$$\boldsymbol{t}_s(s,t_0) = -K(s,t_0)\boldsymbol{n}(s,t_0) \tag{3.46}$$

where

$$K(s,t_0) = (\hat{y}_{ss}\hat{x}_s - \hat{x}_{ss}\hat{y}_s)(s,t_0) \tag{3.47}$$

in the mean curvature. Finally, we introduce the local change of coordinates

$$\boldsymbol{X}(s,\rho) = \hat{\boldsymbol{x}}(s,t_0) + \rho\boldsymbol{n}(s,t_0) \tag{3.48}$$

and note that

$$\boldsymbol{X}_s = (1 + K(s,t_0)\rho)\boldsymbol{t}(s,t_0) \tag{3.49}$$

and

$$\boldsymbol{X}_\rho = \boldsymbol{n}(s,t_0). \tag{3.50}$$

For $|\rho| \ll 1$ and $|t - t_0| \ll 1$ our evolution equation (3.38) takes the form

$$\frac{\delta}{c}p_t = \delta^2 p_{\rho\rho} + \frac{K\delta^2}{(1+K\rho)}p_\rho + \frac{\delta^2}{(1+K\rho)}\frac{\partial}{\partial s}\left(\frac{1}{1+K\rho}\frac{\partial p}{\partial s}\right) + T_0(t)|1-p^2|^{\frac{1+\lambda}{2}} + p|1-p^2|^{\lambda}\ \mathrm{sign}\ (1-p^2). \tag{3.51}$$

Our moving fronts will be approximate solutions of (3.51) of the form:

$$p = \tilde{p}\left(\frac{\rho - \int_{t_0}^{t}\tilde{c}(s,\eta)d\eta}{\delta}\right) \tag{3.52}$$

At $t = t_0$, these approximate solutions satisfy

$$\tilde{p}_{\xi\xi} + K(s,t_0)\delta\tilde{p}_\xi + \frac{\tilde{c}(s,t_0)}{c}\tilde{p}_\xi + T_0(t_0)|1-\tilde{p}^2|^{\frac{1+\lambda}{2}} + \tilde{p}|1-\tilde{p}^2|^{\lambda}\ \mathrm{sign}\ (1-\tilde{p}^2) = 0(\delta^2), \tag{3.53}$$

and the boundary conditions

$$\tilde{p}(-\infty) = -1 \text{ and } \tilde{p}(\infty) = +1. \tag{3.54}$$

If we replace the $0(\delta^2)$ terms on the right hand side of (3.53) by 0, then the analysis of the early part of this section guarantees an approximate profile which satisfies the reduced ansatz

$$\tilde{p}_\xi = |1-\tilde{p}^2|^{\frac{1+\lambda}{2}} \tag{3.55}$$

and this is given by the quadrature formula

$$\int_0^{\tilde{p}(\xi)} \frac{d\eta}{(1-\eta^2)^{\frac{1+\lambda}{2}}} = \xi \quad , \quad -\Omega < \xi < \Omega \tag{3.56}$$

where

$$\Omega = \int_0^1 \frac{d\eta}{(1-\eta^2)^{\frac{1+\lambda}{2}}}. \tag{3.57}$$

For $\xi \le -\Omega, \tilde{p}(\xi) = -1$ and for $\Omega \le \xi, \tilde{p}(\xi) = 1$. The normal velocity, $\tilde{c}(s,t_0) = (\tilde{x}_t(s,t_0), \hat{y}_t(s,t_0)) \cdot \boldsymbol{n}(s,t_0)$, is not arbitrary but satisfies

$$\frac{\tilde{c}(s,t_0)}{c} + K(s,t_0)\delta + T_0(t_0) = 0. \tag{3.58}$$

(3.58) is the Gibbs-Thomson relation for the reduced system (3.38) - (3.42). The oddness of the $\tilde{p}$ profile in ξ implies that for a solution with a single interface $\Gamma(t_0)$ the mean temperature is given by

$$T_0(t_0) = e_{\frac{1+\lambda}{2}}(1)\left(H_0 - 1 + \frac{1}{2}\int_0^{L(t_0)}(\hat{x}\hat{y}_s - \hat{y}\hat{x}_s)(s,t_0)ds\right) \Big/ \iint_\Omega 1dxdy. \tag{3.59}$$

This latter formula is easily modified for solutions with multiple interfaces.

4 Numerical Simulations

In this section we focus on simulations for the one-dimensional system (3.1) - (3.5). For definiteness we choose

$$\gamma = 2 \text{ and } \mu = \lambda = 1/2. \tag{4.1}$$

These parameters are consistent with (3.19) and thus the resulting system supports the moving interface solutions of the previous section. With these parameters we have

$$e_{1/2}(p) \stackrel{def}{=} \int_0^p |1-s^2|^{1/2} ds = \begin{cases} \frac{1}{2}\left(\sin^{-1}(p) + p\sqrt{1-p^2}\right), \ 0 \le p \le 1 \\ \\ \frac{\pi}{4} + \frac{1}{2}\left(p\sqrt{p^2-1} - \cosh^{-1}(p)\right), \ 1 \le p \end{cases} \tag{4.2}$$

and

$$e_{1/2}(p) = -e_{1/2}(-p), \ -\infty < p \le 0. \tag{4.3}$$

and the functional $\mathcal{J}(\cdot)$ defined in (3.7) takes the form:

$$\mathcal{J}(p) = \int_0^1 \left(\frac{\delta^2 |p_x|^3}{3} + \frac{\left|1-p^2\right|^{3/2}}{3\delta}\right)(x,t)dx + \frac{T_0^2(t)}{2\delta} \tag{4.4}$$

where

$$T_0(t) = \frac{\pi}{4}H_0 - \int_0^1 e_{1/2}(p(x,t))dx \tag{4.5}$$

and

$$H_0 = \frac{4}{\pi}\int_0^1 \left(T(x,0^+) + e_{1/2}(p(x,0^+))\right) dx. \tag{4.6}$$

This basic decay estimate for this system follows from the identity

$$-c\frac{d}{dt}\mathcal{J}(p(\cdot,t)) = -cD\mathcal{J}\left(p(\cdot,t)|p_t(\cdot,t)\right) = \int_0^1 p_t^2(x,t)dx, \tag{4.7}$$

which guarantees that

$$\mathcal{J}(p(\cdot,t)) + \frac{1}{c}\int_0^t \left(\int_0^1 p_s^2(x,s)dx\right) ds = \mathcal{J}(p(\cdot,0^+)). \tag{4.8}$$

Finally, for the choice of parameters $(\gamma, \mu, \lambda) = (2, 1/2, 1/2)$ the basic single front profile centered at $x = L(t)$ is of the form:

$$\tilde{p} = \begin{cases} -1, \ x < L(t) - \dfrac{\pi\delta}{2^{2/3}} \\ \\ \sin\left(\dfrac{x - L(t)}{2^{1/3}\delta}\right), \ L(t) - \dfrac{\pi\delta}{2^{2/3}} \leq x \leq L(t) + \dfrac{\pi\delta}{2^{2/3}} \\ \\ 1, \ L(t) + \dfrac{\pi\delta}{2^{2/3}} < x. \end{cases} \tag{4.9}$$

In our numerical simulations we choose

$$\Delta x = 1/500 \text{ and } \delta = \frac{5\Delta x 2^{2/3}}{\pi} = .0050529\ldots. \tag{4.10}$$

With this choice of Δx and δ the basic $-1/+1$ phase transition defined in (4.9) takes place over an interval of length $10\Delta x$.

Our basic computational cells are centered at the grid points

$$x_k = \frac{(2k-1)}{1000} \quad , \quad 1 \leq k \leq 500 \tag{4.11}$$

and the discrete unknowns, $p_k(t)$, denote the approximate values of p at x_k at time t; i.e.

$$p_k(t) \simeq p(x_k, t). \tag{4.12}$$

An alternative interpretation of $p_k(t)$ is as a cell average, namely

$$p_k(t) = 500 \int_{x_k - 1/1000}^{x_k + 1/1000} p(\xi, t) d\xi. \tag{4.13}$$

Using the method of lines, we replace (3.1) with

$$\frac{\delta}{c}\dot{p}_k = (500)^3\delta^3 \left(|p_{k+1} - p_k|(p_{k+1} - p_k) - |p_k - p_{k-1}|(p_k - p_{k-1})\right) + \left(T_0(t) + p_k \text{ sign } (1 - p_k^2)\right) |1 - p_k^2|^{1/2} \tag{4.14}$$

and our implementation of the boundary conditions (3.2) comes from insisting that

$$p_0(t) = p_1(t) \ \text{ and } \ p_{501}(t) = p_{500}(t). \tag{4.15}$$

The mean temperature appearing in (4.14) is computed by

$$T_0(t) = \frac{\pi}{4}H_0 - \frac{1}{500}\sum_{j=1}^{500} e_{1/2}(p_j(t)). \tag{4.16}$$

We note that (4.14) is also a gradient flow, specifically if we let

$$\tilde{J} = \frac{\delta^2(500)^2}{3} \sum_{j=1}^{499} |p_{j+1} - p_j|^3 + \frac{1}{1500\delta} \sum_{j=1}^{500} \left|1 - p_j^2\right|^{3/2} + \frac{T_0^2}{2\delta}, \tag{4.17}$$

then (4.14) may be rewritten as

$$\dot{p}_k = -500c\, \frac{\partial \tilde{\mathcal{J}}}{\partial p_k}. \tag{4.18}$$

The latter identity implies that

$$\tilde{\mathcal{J}}(t) + \frac{1}{500c} \int_0^t \left(\sum_{k=1}^{500} \dot{p}_k^2(s) \right) ds = \tilde{\mathcal{J}}(0).$$

We note that if the constant H_0 in (4.16) satisfies

$$\frac{-4}{\pi} + 1 \leq H_0 \leq \frac{4}{\pi} - 1 \tag{4.19}$$

and the initial data $p_k(0^+) = p_k^0$ satisfies

$$-1 \leq p_k^0 \leq 1 \quad , \quad 1 \leq k \leq 500, \tag{4.20}$$

then the initial temperature

$$T_0^0 \stackrel{def}{=} \frac{\pi H_0}{4} - \frac{1}{500} \sum_{j=1}^{500} e_{1/2}(p_j^0) \tag{4.21}$$

satisfies

$$-1 < T_0^0 < 1. \tag{4.22}$$

If these constraints hold, then the solutions of (4.14) - (4.16) taking on the initial data $p_k(0^+) = p_k^0$, $1 \leq k \leq 500$, satisfy the pointwise bounds

$$-1 \leq p_k(t) \leq 1 \quad \text{and} \quad -1 < T_0(t) = \frac{\pi H_0}{4} - \frac{1}{500} \sum_{j=1}^{500} e_{1/2}(p_k(t)) < 1. \tag{4.23}$$

In all simulations we chose a modified first order Euler scheme to integrate (4.14) with a time step

$$\Delta t = \frac{\Delta x}{100}. \tag{4.24}$$

We also chose $c = 1$ and initial data satisfying (4.20) and (4.22). The specific scheme is given below. We let

$$P_k = p_k^n + \lambda(|p_{k+1}^n - p_k^n|(p_{k+1}^n - p_k^n) - |p_k^n - p_{k-1}^n|(p_k^n - p_{k-1}^n)) + \mu(T_0^n + p_k^n \text{ sign } (1-(p_k^n)^2))|1-(p_k^n)^2|^{1/2} \tag{4.25}$$

where

$$\lambda = \frac{\delta^2 \Delta t}{(\Delta x)^2} = \frac{1}{4^{2/3}\pi^2} \quad \text{and} \quad \mu = \frac{\Delta t}{\delta} = \frac{\pi}{500 \cdot 2^{2/3}}. \tag{4.26}$$

The updates, p_k^{n+1}, are then given by

$$p_k^{n+1} = \begin{cases} -1, & \text{if } P_k < -1 \\ P_k, & \text{if } -1 \le P_k \le 1 \\ 1, & \text{if } P_k > 1. \end{cases} \tag{4.27}$$

We note that the diffusive portion of the update, namely the term

$$\tilde{P}_k = p_k^n + \lambda \left(\left|p_{k+1}^n - p_k^n\right| \left(p_{k+1}^n - p_k^n\right) - \left|p_k^n - p_{k-1}^n\right| \left(p_k^n - p_{k-1}^n\right) \right) \tag{4.28}$$

may be rewritten as

$$\tilde{P}_k = \left(1 - \lambda \left|p_{k+1}^n - p_k^n\right| - \lambda \left|p_k^n - p_{k-1}^n\right|\right) p_k^n + \lambda \left|p_k^n - p_{k-1}^n\right| p_{k-1}^n + \lambda \left|p_{k+1}^n - p_k^n\right| p_{k+1}^n \tag{4.29}$$

and this latter identity and (4.26), implies that if $-1 \le p_j^n \le 1, \; 1 \le j \le 500$, then

$$0 \le \lambda \left|p_{k+j}^n - p_{k-1+j}^n\right| \le \frac{1}{2^{1/3}\pi^2} = .0804187\ldots \quad , \quad j = 0, 1, \tag{4.30}$$

and thus the diffusive portion of the update satisfies

$$-1 \le \tilde{P}_k \le 1. \tag{4.31}$$

Moreover, the smallness of μ implies that the P_k's defined in (4.25) can violate the upper and lower bounds in a single iteration by a negligible amount.

All simulations were run with the constant $H_0 = 0$. To check our code we conducted tests with the initial data

$$p_k(x, 0^+) = -\cos(2^{k-1}\pi x) \quad , \quad k = 1, 2, 3. \tag{4.32}$$

The k^{th} data yielded stationary interfaces located at

$$L_{k,j} = \frac{(2j-1)}{2^k} \quad , \quad 1 \le j \le 2^{k-1}. \tag{4.33}$$

The top frame in each of Figures 1-3 shows the computed equilibrium profile starting from the data $(4.32)_k$ and the bottom frame shows a blowup of the computed profile and also a plot of the theoretical equilibrium profile, $\sin\left(\frac{x - L_{k,1}}{2^{\frac{1}{3}}\delta}\right)$, over the interval

$$L_{k,1} - 5\Delta x \leq x \leq L_{k,1} + 5\Delta x.$$

The computed profiles are in blue and the theoretical profiles are in green. The reader will note that these overlay each other and are indistinguishable.

5 Conclusions

The author believes that the class of models developed in this paper has many strengths not shared by the classical "phase-field" models. In particular when describing planar melt/solidification problems our model supports stable equilibria which represent slabs of ice interspersed between wet regions, all at the constant melt temperature. No such solutions are supported by classical "phase-field" models. Since similar solutions are supported by sharp-interface theories of melting and solidification it is clear that the models presented here are better candidates for regularizations of the sharp interface model than the classic "phase-field" model, i.e. for regularizations which yield the observed solutions of the sharp-interface model in the $\delta = 0^+$ limit.

References

1. Caginalp, G., "An analysis of a phase-field model of a free boundary," Arch. Rat. Mech. Anal. 92 (1986) 205-245.

2. Caginalp, G., "Stefan and Hele-Shaw Type Models as Asymptotic Limits of the Phase Field Equation," Phys. Rev. A 39 (1989) 5887-5896.

3. Caginalp, G., "Phase Field Models and Sharp Interface Limits: Some Differences in Subtle Situations," Rocky Mountain J. Math. 21 (1996), 2, 603-616.

4. Caginalp, G. and X. Chen, "Phase Field Equations in the Singular Limit of Sharp Interface Problems", IMA Volume 43, "On the Evolution of Phase Boundaries", 1990-91, pp. 1-28.

5. Caginalp, G. and E. Sokolovsky, "Phase Field Computations of Single-Needle Crystals, Crystal Growth, and Motion by Mean Curvature", SIAM J. Sci. Comput., 15, 1, pp. 106-126 (1994).

6. Fabbri, M. and V.R. Vollmer, "The phase-field method in the sharp-interface limit: A comparison between model potentials," Jour. Comp. Physics 130 (1997), 256-265.

7. McFadden, G.B., A.A. Wheeler, R.J. Brown, S.R. Coriell and R.F. Sekerka, "Phase-Field odels for Anisotropic Interfaces," Phys. Rev. E 48 (1993) 2016-2024.

8. Wang, S.L., R.F. Sekerka, A.A. Wheeler, B.T. Murray, S.R. Coriell, R.J. Braun, and G.B. McFadden, "Thermodynamically-Consistent Phase-Field Models," Physica D 69 (1993) 189-200.

9. Wang, S.L. and R.F. Sekerka, “Algorithms for Phase Field Computations of the Dendritic Operating State at Large Supercoolings,” J. Comp. Physics 127 (1996) 110-117.

10. Greenberg, J.M., “Estimates and Computations for Melting and Solidification Problems, Math. Modelling and Num. Anal., 35, 4 (2001), 607-631.

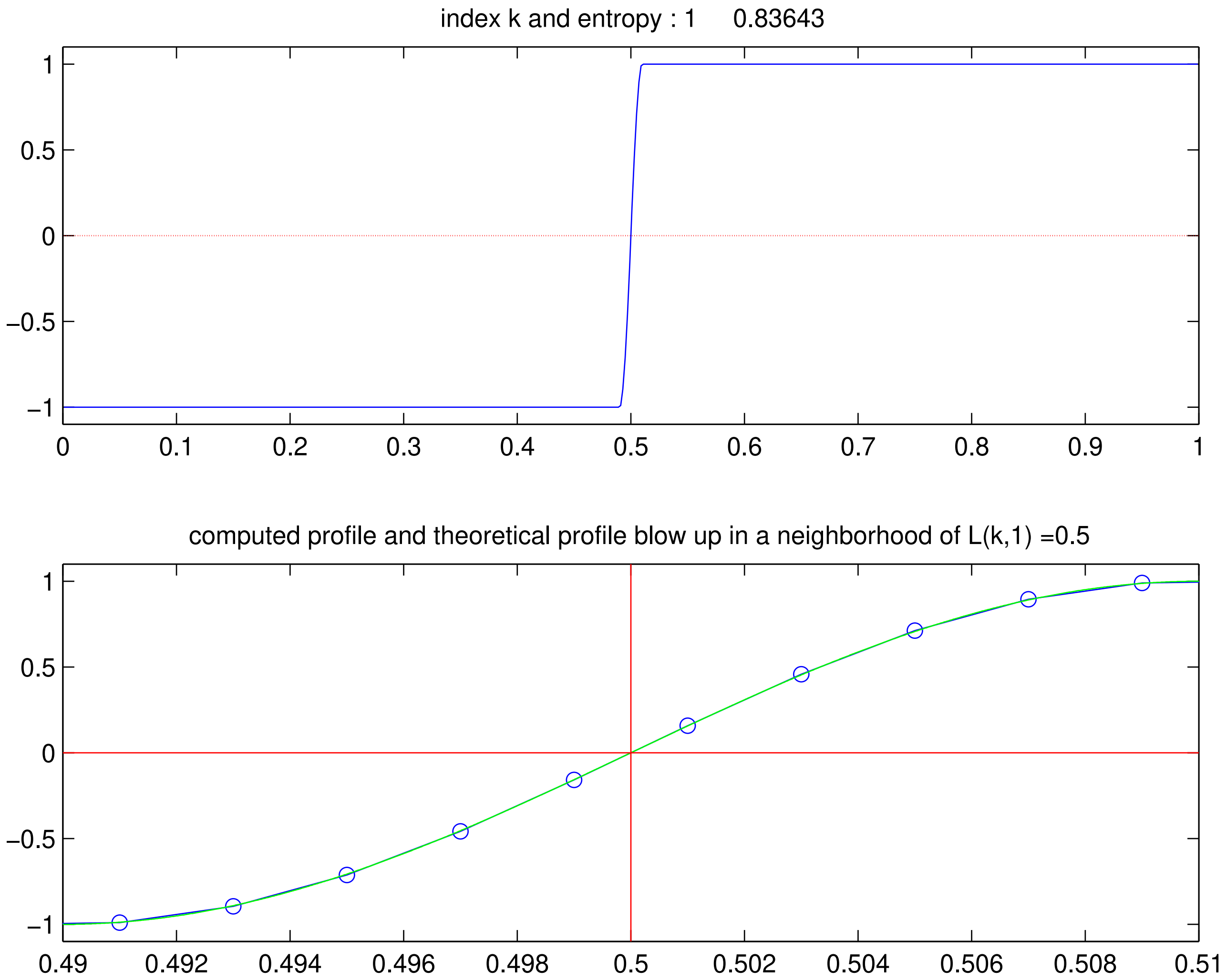
index k and entropy : 1 0.83643
1
0.5
0
−0.5
−1
0
0.1
0.2
0.3
0.4
0.5
0.6
0.7
0.8
0.9
1
computed profile and theoretical profile blow up in a neighborhood of L(k,1) =0.5
1
0.5
0
−0.5
−1
0.49
0.492
0.494
0.496
0.498
0.5
0.502
0.504
0.506
0.508
0.51

Figure 1

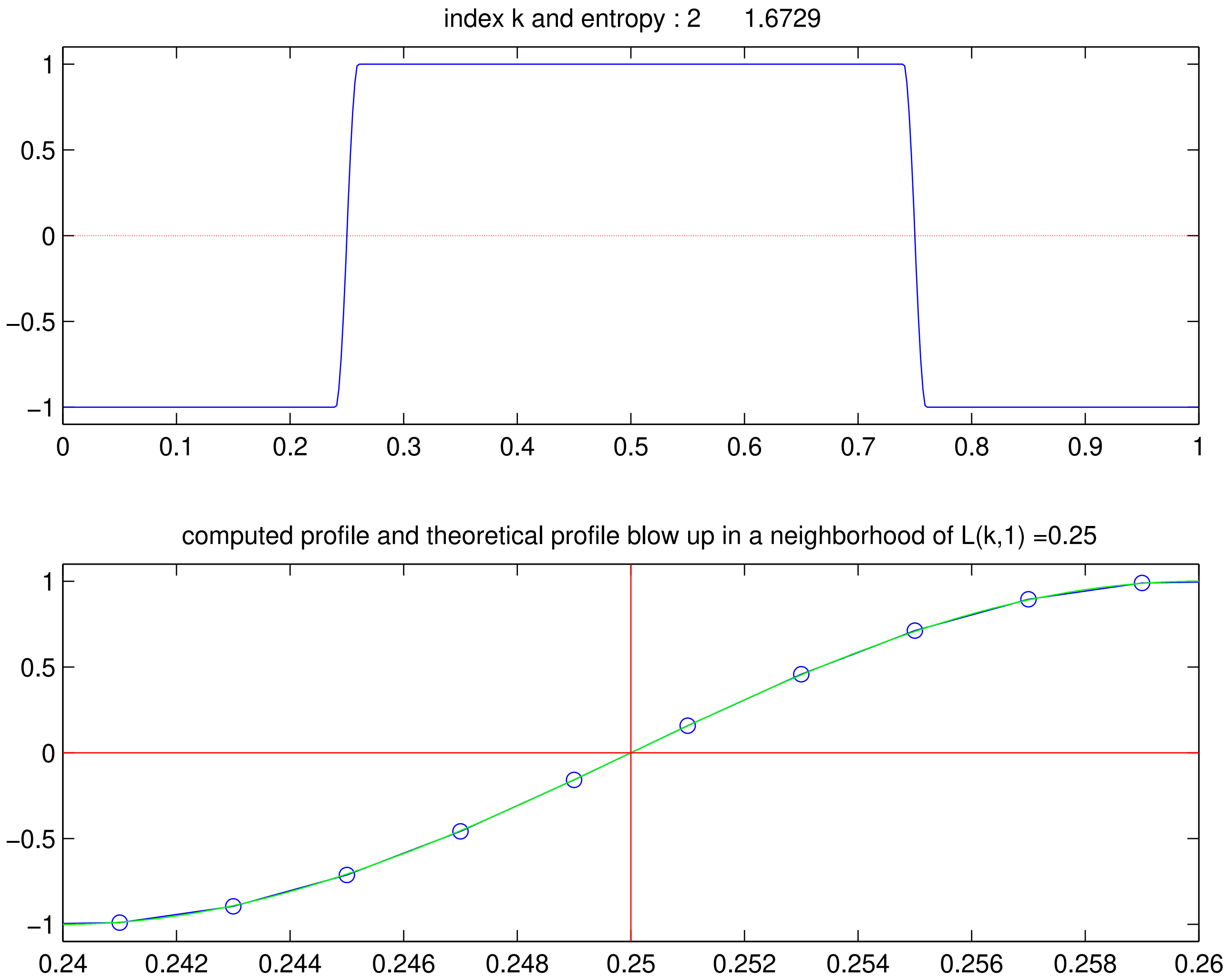
index k and entropy : 2 1.6729
1
0.5
0
−0.5
−1
0
0.1
0.2
0.3
0.4
0.5
0.6
0.7
0.8
0.9
1
computed profile and theoretical profile blow up in a neighborhood of L(k,1) =0.25
0.24
0.242
0.244
0.246
0.248
0.25
0.252
0.254
0.256
0.258
0.26

Figure 2

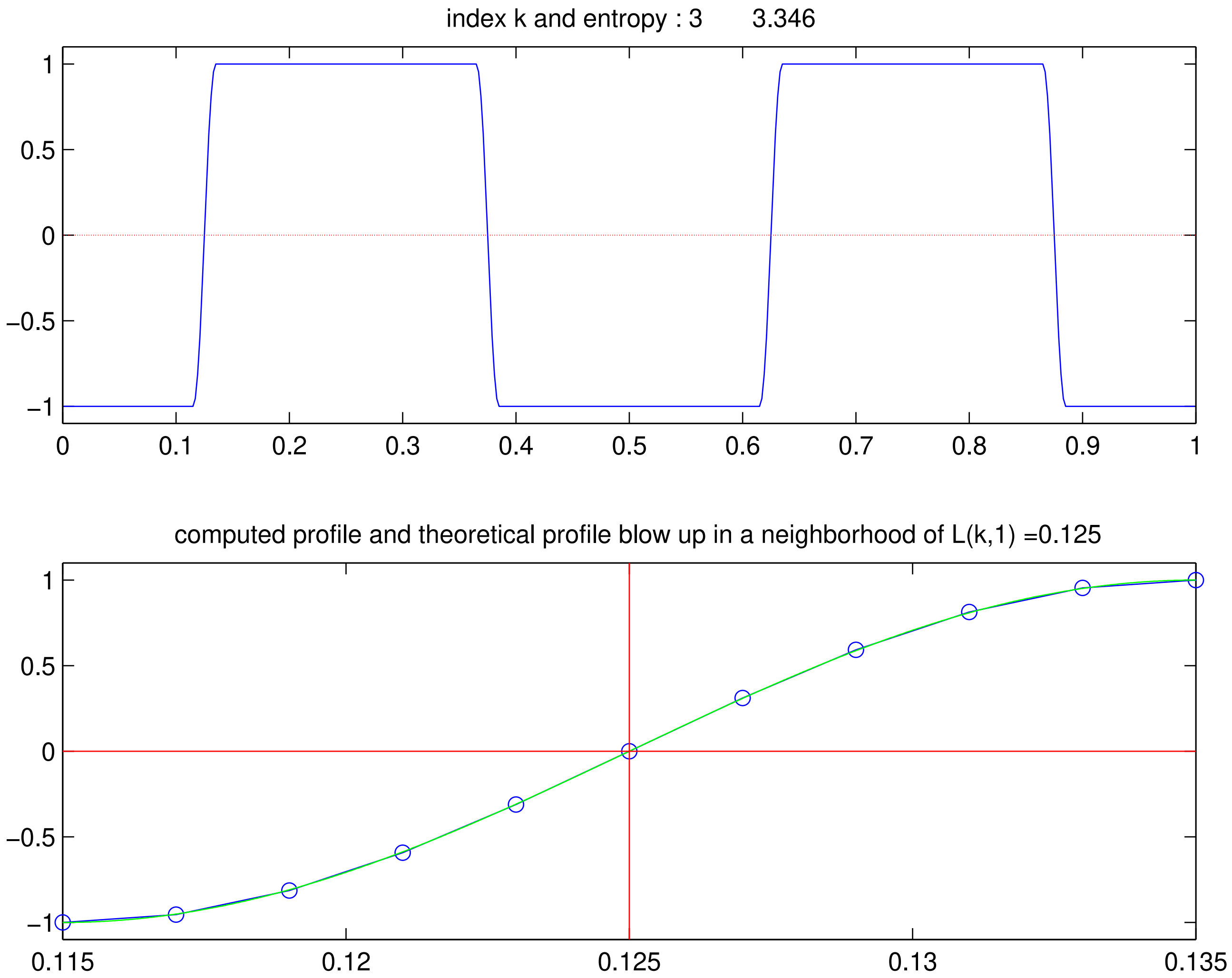
index k and entropy : 3 3.346
1
0.5
0
−0.5
−1
0
0.1
0.2
0.3
0.4
0.5
0.6
0.7
0.8
0.9
1
computed profile and theoretical profile blow up in a neighborhood of L(k,1) =0.125
1
0.5
0
−0.5
−1
0.115
0.12
0.125
0.13
0.135

Figure 3